J. Plasma Physics (2007), *vol.* 73, *part* 5, *pp.* 731–740. © 2006 Cambridge University Press
doi:10.1017/S0022377806006192 First published online 10 November 2006 Printed in the United Kingdom

Collisionless trapped-electron-mode turbulence and transport in fluid descriptions

H. NORDMAN[1], P. STRAND[1] and X. GARBET[2]

[1]Department of Radio and Space Science, Chalmers University of Technology, Euratom-VR Association, SE-412 96 Göteborg, Sweden (elfhn@chalmers.se)

[2]Association Euratom-CEA, CEA/DSM/DRFC CEA-Cadarache, France

(Received 31 August 2006)

Abstract. A study of particle and electron heat transport in tokamaks due to trapped-electron-mode (TEM) turbulence is presented. The study is based on the Weiland fluid model for ion-temperature-gradient (ITG) modes and TEMs, complemented and compared with a trapped electron fluid treatment which retains contributions from the weakly trapped electrons. The dependence of the fluid transport coefficients on magnetic shear and other plasma parameters is discussed and compared with results obtained from nonlinear gyrokinetic simulations. Inward (pinch) flows of particles and heat, previously reported for the coupled ITG–TEM system, are also found in the TEM dominated regime.

1. Introduction

The anomalous transport of particles and heat observed in magnetic fusion devices is generally attributed to turbulence driven by short-wavelength drift-type instabilities [1]. The two main instabilities considered for the hot core region of tokamak plasmas are the toroidal ion-temperature-gradient (ITG) mode [2] and the collisionless trapped electron mode (TEM) [3]. First principles transport models based on advanced fluid descriptions of these instabilities are now widely used in predictive transport code simulations and in the analysis of tokamak discharges [4–6]. While a substantial effort has been devoted to the development and refinement of the ITG-driven transport models by utilizing advanced fluid and kinetic treatments (see, e.g., [7] and references therein), much less work has been devoted to the study of TEM driven transport.

However, a number of recent quasilinear and nonlinear gyrokinetic investigations of transport driven by TEM turbulence have been reported [8–10]. The TEM dominated regime is relevant to tokamak experiments with dominant central electron heating [10–12] where the ions are rather cold and the ITG modes are stable. This regime is well suited for a comparison of fluid descriptions of TEM transport with more advanced kinetic descriptions as part of the development of more accurate and efficient models for the analysis and prediction of plasma discharges.

In the present work, the Weiland fluid model [13] for ITG–TEM transport, complemented with a trapped electron (TE) fluid treatment [14] retaining contributions from the weakly TEs to the bounce-averaged TE equations, is used to calculate

https://doi.org/10.1017/S0022377806006192 Published online by Cambridge University Press

particle and heat transport in the TEM dominated regime. The investigation is focused on pure TEM turbulence by considering the limit $R/L_{T\mathrm{i}} = 0$ and $T_\mathrm{e} > T_\mathrm{i}$ where the ITG physics are suppressed. The dependence of TEM transport on magnetic shear and other plasma parameters is discussed and a preliminary qualitative comparison with nonlinear gyrokinetic simulation results for TEM transport [8] is presented. It is found that the fluid treatments are able to qualitatively reproduce a majority of the kinetic scalings when the shear dependence of the bounce-averaged magnetic drift frequency is retained. Parameter scalings where the results of the kinetic and fluid treatments differ are discussed. In the fluid treatments, the presence of particle and heat pinch flows, as previously reported for the coupled ITG–TE system, is found also in the TEM-dominated regime.

The remainder of the paper is organized as follows. In Sec. 2, the fluid models used for the study of TE-driven transport are briefly summarized. Section 3 presents the transport results and a qualitative comparison with kinetic simulation results. Finally, in Sec. 4 the summary and conclusions are given.

2. Fluid description

The original formulation of the Weiland transport model [13] is used here, in the electrostatic limit, for the description of ions and deeply TEs. It is complemented by a TE fluid treatment [14] which includes contributions to the bounce-averaged magnetic drifts from weakly TEs.

The fluid models have been described in detail elsewhere and therefore only a brief summary is given here, with particular emphasis on the treatment of TEs. Each species is described by the continuity, parallel momentum and energy equations for the perturbations in density, parallel velocity and pressure. The ion and TE fluid models are symmetric, except that the parallel velocity perturbation is zero for the bounce-averaged TE fluid, and electron finite-Larmor-radius (FLR) effects can be neglected. In the TE fluid treatment [14], the electron magnetic drift is, after the bounce averaging, replaced by the precession frequency of TEs as $\langle \omega_{D_\mathrm{e}} \rangle = \omega_{D_\mathrm{e}} \cdot \lambda_\mathrm{t}$ where $\omega_{D_\mathrm{e}} = 2k_\theta \rho_s c_s/R$ and the parameter $\lambda_\mathrm{t} = 1/4 + s \cdot 2/3$ characterizes the dependence of the precession frequency on the magnetic shear s. The original formulation of the Weiland model for deeply TE is recovered for $\lambda_\mathrm{t} = 1$. We note that the two TE fluid models are identical for a magnetic shear of $s = 9/8$ ($\lambda_\mathrm{t} = 1$), but may differ substantially for $s < 1$ and $s > 1$. The free electrons are assumed to be Boltzmann distributed. The ion and electron perturbations are coupled through the quasi-neutrality condition $\delta n_\mathrm{i}/n_\mathrm{i} = f_t \delta n_\mathrm{et}/n_\mathrm{et} + (1 - f_\mathrm{t})\delta n_\mathrm{ef}/n_\mathrm{ef}$, where f_t is the fraction of trapped electrons. The resulting eigenvalue equation is then reduced to a set of five coupled algebraic equations by assuming a strongly ballooning eigenfunction. The coupled system of five algebraic equations describes ITG modes, driven by R/L_{T_i} and suppressed by R/L_n, and collisionless TE modes driven by both R/L_{T_e} and R/L_n. If the influence of parallel ion dynamics on the TE mode physics is neglected (see Sec. 3 for a discussion of this), a further reduction of the system to four algebraic equations is possible.

The corresponding transport coefficients, calculated using quasilinear theory and a modified mixing length estimate and supported by nonlinear fluid simulations of ITG–TEM turbulence [15], can be written as

$$D = f_\mathrm{t} \Delta_n \frac{\gamma^3/k_x^2}{\omega_{*_\mathrm{e}}^2}, \tag{1a}$$

https://doi.org/10.1017/S0022377806006192 Published online by Cambridge University Press

$$\chi_{\rm e} = f_{\rm t}\frac{1}{\eta_{\rm e}}\left(\eta_{\rm e} - \frac{2}{3} - \frac{2}{3}\Delta_{\rm e}\right)\frac{\gamma^3/k_x^2}{(\omega_r - 5\langle\omega_{D_{\rm e}}\rangle/3)^2 + \gamma^2}, \tag{1b}$$

where $f_{\rm t} = \sqrt{2\varepsilon/(1+\varepsilon)}$ is the fraction of TEs, $\varepsilon = r/R$, $\eta_{\rm e} = L_n/L_{T_{\rm e}}$, $\omega = \omega_r + i\gamma$ is the eigenvalue, $\omega_{*_{\rm e}} = k_\theta \rho_s c_s/L_n$ is the diamagnetic drift frequency and $\langle\omega_{D_{\rm e}}\rangle = \omega_{D_{\rm e}}\lambda_{\rm t} = (2k_\theta\rho_s c_s/R)\lambda_{\rm t}$ is the bounce-averaged magnetic drift frequency. The parameters Δ_j are phase shifts which are complex functions of the eigenvalues and profile shape parameters [13]. The space scale of the turbulence is fixed by choosing $(k_x\rho_s)^2 = (k_\theta\rho_s)^2 = 0.1$, corresponding to the scale of the fastest growing mode.

In the following, pure TEM transport will be studied by considering the case $R/L_{T_{\rm i}} = 0$ and $T_{\rm e} > T_{\rm i}$ where the ITG mode is suppressed. In this limit, a simple analytical estimate of the particle flux can be obtained from the ion physics and the ambipolarity condition $\Gamma_{n_{\rm e}} = \Gamma_{n_{\rm i}}$. The ion particle flux $\Gamma_{n_{\rm i}} = \langle\nu_{E_x}\delta n_{\rm i}\rangle$ is calculated from the ion density response [13] (neglecting parallel ion dynamics)

$$\frac{\delta n_{\rm i}}{n_{\rm i}} = \omega_{*_{\rm e}}\frac{\omega(1-\varepsilon_n) - (7/3 - \eta_{\rm i} - 5\varepsilon_n/3)\omega_{D_{\rm i}} + FLR}{\omega^2 - 10\omega\omega_{D_{\rm i}}/3 + 5\omega_{D_{\rm i}}^2/3}\frac{e\phi}{T_{\rm e}}, \tag{2}$$

where $\varepsilon_n = 2L_n/R$, $\eta_{\rm i} = L_n/L_{T_{\rm i}}$, $\omega_{D_{\rm i}} = -\omega_{D_{\rm e}}T_{\rm i}/T_{\rm e}$ is the ion magnetic drift frequency and FLR represents contributions from ion inertia and ion FLR effects. Assuming $T_{\rm i}/T_{\rm e} \ll 1$ and $k^2\rho_{s,{\rm i}}^2 \ll 1$, and using Fick's law $D = \Gamma_{n_{\rm i}}L_n/n_{\rm i}$, the diffusion coefficient takes the simple form

$$D_{\rm e} = D_{\rm i} \approx (1-\varepsilon_n)\frac{\gamma^3/k_x^2}{|\omega|^2}. \tag{3}$$

This simple analytical estimate confirms the presence of a particle pinch for $\varepsilon_n > 1$ ($R/L_n < 2$), provided the TEM is unstable in this region (i.e. for a sufficiently flat density profile combined with a steep electron temperature gradient).

3. Parameter scalings of transport

In the following, the quasilinear particle and electron heat transport due to TEMs will be calculated numerically using the transport expressions in (1a), (1b) and (3), and the resulting scalings will be compared qualitatively with recent nonlinear and quasilinear kinetic results [8–10]. For the TE fluid treatment, the two models ($\lambda_{\rm t} = 1$ and $\lambda_{\rm t} = 1/4 + s\cdot 2/3$, respectively) will be compared. The main difference between the fluid treatments can be expected in the magnetic shear scaling of transport which is treated first. Then, scalings with R/L_n, $R/L_{T_{\rm e}}$ and safety factor q will be discussed. For these scalings, similar results can be expected from the two TE treatments (for $s \approx 1$) and hence only results obtained for $\lambda_{\rm t} = 1/4 + s\cdot 2/3$ will be presented. The set of parameters used are taken mainly from the nonlinear kinetic investigation [8] with $T_{\rm e}/T_{\rm i} = 3$, $R/L_{T_{\rm i}} = 0$ ($\eta_{\rm i} = 0$), $R/L_{T_{\rm e}} = 3$, $R/L_n = 3$, $f_{\rm t} = 0.52$ ($\varepsilon = 0.16$), $q = 1.4$, $s = 0.8$ and $\beta_{\rm e} = 0$. In the kinetic study, electromagnetic perturbations were also included. However, the low value of β used ($\beta_{\rm e} = 0.001$) would not modify the electrostatic results presented here.

3.1. Magnetic shear

In Fig. 1 the particle and heat diffusivities as a function of magnetic shear s are displayed. The results are shown for the original Weiland model for deeply trapped particles ($\lambda_{\rm t} = 1$, circles) and for the model including bounce-averaged magnetic

https://doi.org/10.1017/S0022377806006192 Published online by Cambridge University Press

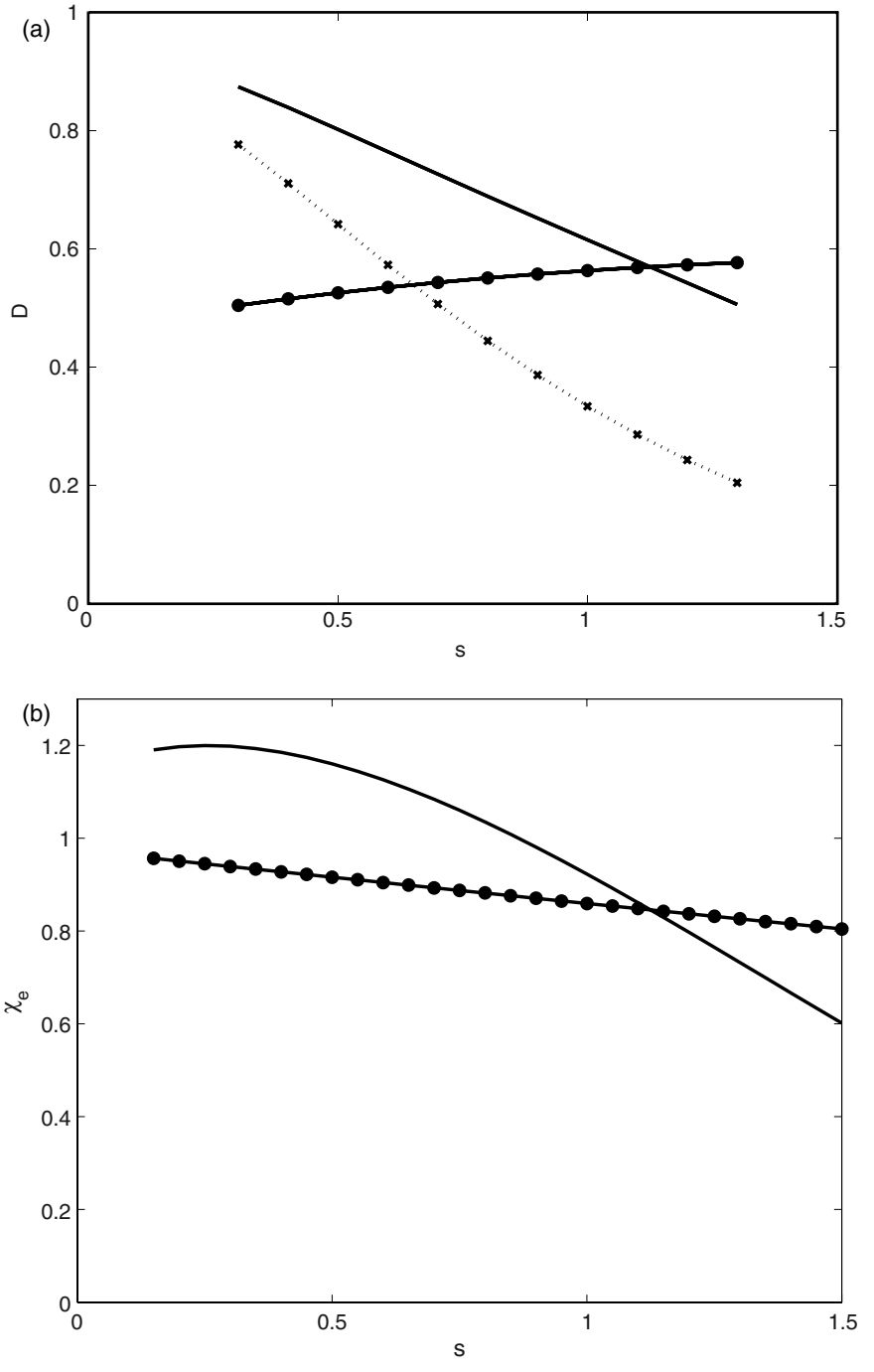


Figure 1. (a) Particle diffusivity and (b) electron heat diffusivity (in units of $2\rho_s^2 c_s/R$) as a function of magnetic shear s for the bounce-averaged TE model ($\lambda_t = 1/4 + s \cdot 2/3$, solid line) and for the original Weiland model ($\lambda_t = 1$; circles. Also shown in (a) is the analytical solution from (3) (crossed line).

https://doi.org/10.1017/S0022377806006192 Published online by Cambridge University Press

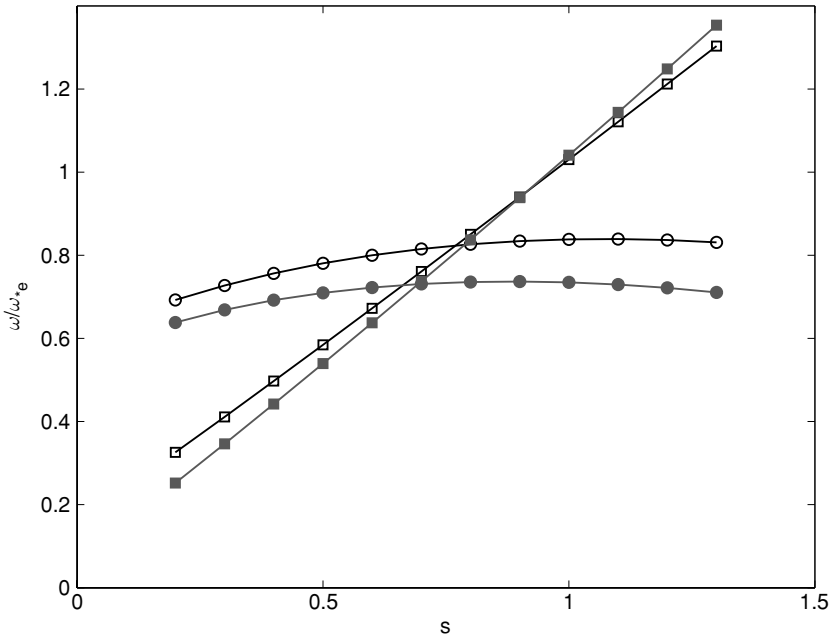


Figure 2. TEM real frequencies (squares) and growth rates (circles) as a function of magnetic shear s for the same parameters as in Fig. 1. The results presented with open squares/circles neglect the effects of parallel ion dynamics.

drift effects ($\lambda_t = 1/4 + s \cdot 2/3$, solid line). As observed, the magnetic shear scaling is dominated by the magnetic drift effects (solid line) whereas the shear dependence in the original Weiland model, originating mainly from the effects of FLR and parallel ion dynamics, is very weak. We note that the TE models give identical results for $s = 9/8$ ($\lambda_t = 1/4 + s \cdot 2/3 = 1$). For negative values of magnetic shear (not covered in Fig. 1), the $\lambda_t = 1/4 + s \cdot 2/3$ model predicts a stabilization of the TEM as the electron precession frequency changes sign [16]. The results in Fig. 1 (solid line) are in good qualitative agreement with the shear scaling reported in the kinetic treatment of [8] (their Fig. 15). We note that the reduction of transport with magnetic shear is reproduced by the simple analytical estimate of the particle diffusivity in (3) (crossed line).

The corresponding linear TEM eigenvalues, including/excluding effects of parallel ion dynamics, are displayed in Fig. 2. As indicated, the TEM growth rate scales weakly with magnetic shear for $s > 0.2$. The shear scaling of particle transport in this region is mainly a result of an increase of the real frequency, which leads to a suppression of the particle flux in accordance with (3). In addition, the two-dimensional (2D) model (neglecting parallel ion dynamics) is able to reproduce the eigenvalues. The results indicate that the effects of parallel ion dynamics on the TEM physics are very weak in the TE-dominated regime, and hence a 2D model may be appropriate.

3.2. Density gradient

The scaling of the particle and heat diffusivities with the normalized density gradient R/L_n, and with R/L_{T_e} as a parameter, is shown in Figs 3(a) and 3(b). The

https://doi.org/10.1017/S0022377806006192 Published online by Cambridge University Press

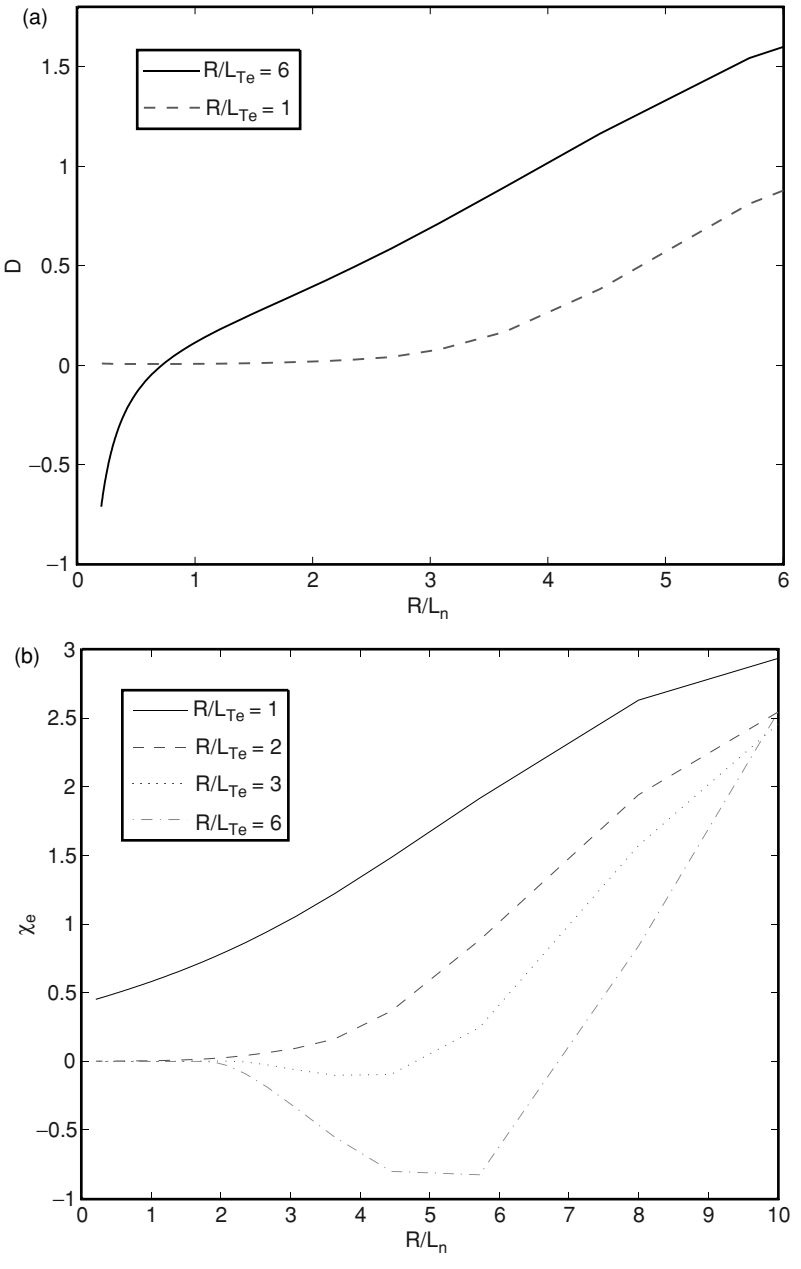


Figure 3. (a) Particle diffusivity and (b) electron heat diffusivity (in units of $2\rho_s^2 c_s/R$) as a function of normalized density gradient R/L_n for (a) $R/L_{T_e} = (1 \text{ and } 6)$ and (b) $R/L_{T_e} = (1, 2, 3 \text{ and } 6)$ with $\lambda_t = 1/4 + s \cdot 2/3$.

standard set of parameters are used with $\lambda_t = 1/4 + s \cdot 2/3$. As expected, the particle diffusivity is found to increase with increasing density gradient. The results in Fig. 3(a) are in qualitative agreement with the kinetic results for $R/L_n > 2$ [8]. For a sufficiently flat density profile ($R/L_n \leqslant 1$) and peaked temperature profile ($R/L_{T_e} = 6$), the non-diagonal terms in the transport matrix dominate and a

https://doi.org/10.1017/S0022377806006192 Published online by Cambridge University Press

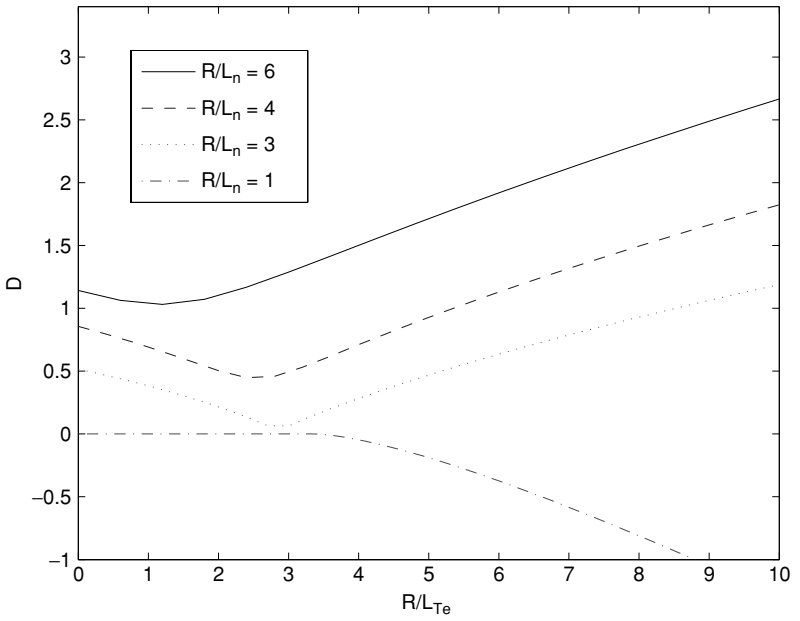


Figure 4. Particle diffusivity (in units of $2\rho_s^2 c_s/R$) as a function of normalized temperature gradient R/L_{T_e} for $R/L_n = (1, 3, 4 \text{ and } 6)$ with $\lambda_t = 1/4 + s \cdot 2/3$.

particle pinch is obtained. The result is consistent with the analytical prediction of (3) of a particle pinch for $R/L_n < 2$. The discrepancy in the threshold value in the parameter R/L_n for obtaining pinch flows can be attributed to the assumption of cold ions used in deriving (3), whereas the standard set of parameters have $T_e/T_i = 3$. The presence of a particle pinch is not reported in the kinetic investigations. It is known from similar studies of ITG-driven transport that the fluid truncation used here gives a stronger tendency for particle pinch flows than kinetic and gyrofluid treatments [17].

The corresponding, and to some extent symmetrical, results for the electron heat diffusivity are given in Fig. 3(b). We note that a heat pinch is obtained for weak temperature gradients ($R/L_{T_e} \leqslant 2$), provided the density gradient is sufficiently steep ($R/L_n \geqslant 2$). The nonlinear kinetic investigation [8] does not cover the region of parameter space where a heat pinch would be expected to be strong according to the present analysis. The kinetic result also shows a saturation of the heat flux for sufficiently steep density gradients which is not reproduced by the fluid models considered here.

3.3. Electron temperature gradient

In Fig. 4 the particle diffusivity as a function of normalized temperature gradient R/L_{T_e} is shown with R/L_n as a parameter. The TE model with $\lambda_t = 1/4 + s \cdot 2/3$ is used. For small values of R/L_{T_e}, the TEM is driven by the density gradient and stabilized by the electron temperature gradient. For larger values of R/L_{T_e}, the drive from the temperature gradient is added. This scaling is well known from various kinetic studies [8–10]. Again, the particle diffusivity is found to increase with R/L_n and a particle pinch is recovered for flat density profiles ($R/L_n < 2$) and for sufficiently steep temperature gradients.

https://doi.org/10.1017/S0022377806006192 Published online by Cambridge University Press

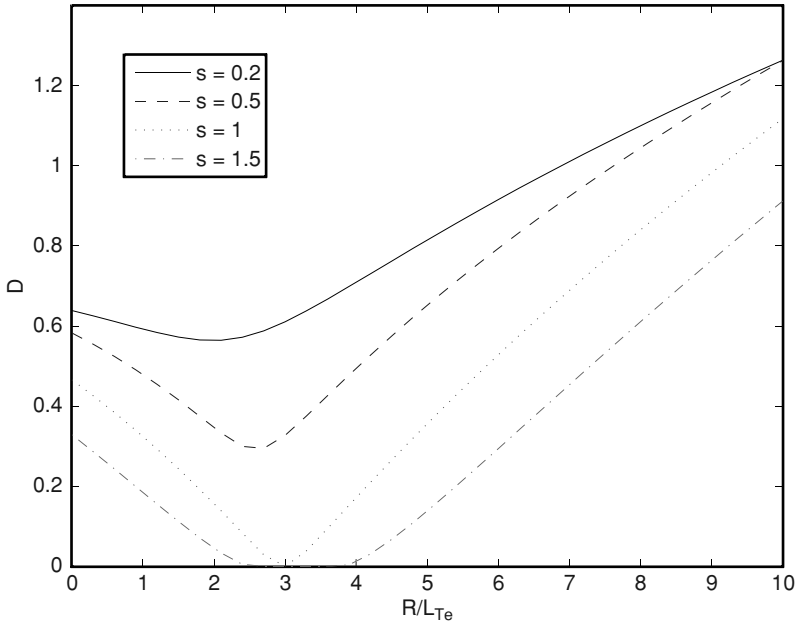


Figure 5. Particle diffusivity (in units of $2\rho_s^2 c_s/R$) as a function of normalized temperature gradient R/L_{T_e} for $s = (0.2, 0.5, 1.0 \text{ and } 1.5)$ with $\lambda_t = 1/4 + s \cdot 2/3$.

Figure 5 displays the particle diffusivity as a function of normalized temperature gradient R/L_{T_e} with magnetic shear s as a parameter. Similar results are obtained for the heat diffusivity. The results are obtained with the bounce-averaged magnetic drift model ($\lambda_t = 1/4 + s \cdot 2/3$). The shear reduction of transport, observed for all values of R/L_{T_e} in this parameter regime, was also seen in the quasilinear kinetic study [10]. The reduction is mainly caused by an increase in the real frequency with magnetic shear and a corresponding suppression of the particle transport, as discussed in connection with Fig. 1. We have verified that the original Weiland model ($\lambda_t = 1$) displays a very week shear scaling in this parameter regime.

3.4. Other scalings

The scaling of the particle and heat diffusivities with safety factor q has also been investigated. A weak increase of the diffusivities with q is found. This is consistent with results obtained using quasilinear kinetic theory [10], whereas the nonlinear kinetic investigation [8] reports a strong q scaling with $\chi_e = q^{1.7}$. Experimentally, the heat diffusivity is found to increase with q to the power 1–2. One reason for the weak q-scaling presented here is the use of a fixed scale for the turbulence with $k_\theta \rho_s = 0.33$, corresponding to the fastest growing mode. The nonlinear kinetic result indicates a shift of the peak of the transport spectrum towards lower mode numbers for increasing values of q, mainly due to Landau resonances. We have verified that the inclusion of a parameter-dependent correlation length [18] in (1a) and (1b) results in a somewhat stronger q scaling, although not as strong as experimentally observed. A similar result is obtained if a spectrum of modes is included in the transport calculations.

https://doi.org/10.1017/S0022377806006192 Published online by Cambridge University Press

4. Summary and conclusions

Particle and electron heat transport driven by collisionless TEM turbulence in fluid descriptions was investigated using both the Weiland fluid model for deeply TEs [13] and a TE fluid model which includes contributions from weakly TEs to the bounce-averaged magnetic drifts [14]. The scaling of the transport coefficients with plasma parameters was also qualitatively compared with nonlinear [8] and quasilinear [9, 10] gyrokinetic results. The TE fluid models, which are identical for a magnetic shear of $s = 9/8$, displayed significant differences in their shear dependence, indicating that the main shear dependence of TEM transport originates from the bounce-averaged magnetic drifts. The kinetic shear scaling [8] of the TEM-driven transport coefficients was well captured by the TE fluid model that retains the shear dependence of the electron precession frequency, whereas for the Weiland model the shear dependence was shown to be very week. In addition, the scaling of transport fluxes with normalized density and temperature gradients (R/L_n, R/L_{T_e}) was generally well reproduced qualitatively by the fluid treatments, except for the very high-density-gradient regime where the kinetically obtained heat diffusivity was found to saturate.

The fluid models predict particle pinches (inward flows) for sufficiently flat density profiles combined with steep electron temperature profiles. Electron heat pinches are obtained in the opposite limit. The possibility of pinch flows was not reported in the kinetic investigations of TEM transport. This may be a result of the linear wave–particle resonances which are known to reduce the pinch flows in gyrokinetic and gyrofluid treatments when compared with the fluid truncation used in the present study [17]. The superlinear scaling of the electron heat diffusivity with safety factor q, reported in the nonlinear kinetic study [8], was not well reproduced in the fluid treatments where a weaker scaling with q was found. This may be a reflection of the neglect of Landau resonances, and the associated shift in the peak of the nonlinear transport spectrum, in the fluid treatments.

The present work studied fluid treatments of TEMs by focusing on pure TEM stability and transport in regions where the ITG mode is linearly stable. Work is under way to include the impact of the TE modelling on the coupled ITG–TEM system with respect to particle pinch flows and mode stability in regions of negative shear.

Acknowledgements

The authors wish to thank Dr L.-G. Eriksson and Professor J. Weiland for valuable discussions and comments.

References

[1] Liewer, P. C. 1985 *Nucl. Fusion* **25**, 543.
[2] Coppi, B. and Pegoraro, F. 1977 *Nucl. Fusion* **17**, 969.
[3] Liu, C. S. 1969 *Phys. Fluids* **12**, 1489.
[4] Strand, P., Nordman, H., Weiland, J. and Christiansen, J. 1998 *Nucl. Fusion* **38**, 545.
[5] Bateman, G., Kritz, A. H., Kinsey, J., Redd, A. and Weiland, J. 1998 *Phys. Plasmas* **5**, 1793.
[6] Parail, V. et al. 1997 *Nucl. Fusion* **37**, 481.
[7] Dimits, A. M. et al. 2000 *Phys. Plasmas* **7**, 969.

https://doi.org/10.1017/S0022377806006192 Published online by Cambridge University Press

[8] Dannert, T. and Jenko, F. 2005 *Phys. Plasmas* **12**, 072 309.
[9] Ernst, D. R. et al. and the Alcator C-Mod Group. 2004 *Phys. Plasmas* **11**, 2637.
[10] Peeters, A. G., Angioni, C., Apostoliceanu, M., Jenko, F., Ryter, F. and the ASDEX Upgrade Team. 2005 *Phys. Plasmas* **12**, 022 505.
[11] Ryter, F. et al. and the ASDEX Upgrade Team. 2003 *Nucl. Fusion* **43**(11), 1396–1404.
[12] Angioni, C., Peeters, A. G., Apostolicearu, M., Jenko, F., Ryter, F. and the ASDFX Update Team. 2005 *Phys. Plasmas* **12**, 040 701.
[13] Weiland, J. 2000 *Collective Modes in Inhomogeneous Plasmas*. Bristol: IOP.
[14] Garbet, X., Garzotti, L., Mantica, P., Nordman, H., Valovic, M. and Weisen, H. 2003 *Phys. Rev. Lett.* **91**, 035001-1.
[15] Nordman, H., Weiland, J. and Jarmen, A. 1990 *Nucl. Fusion* **30**, 983.
[16] Baranov, Yu. F. et al. 2004 *Plasma Phys. Control. Fusion* **46**, 1181.
[17] Eriksson, A., Garzotti, L. and Weiland, J. Private communication.
[18] Weiland, J. and Holod, I. 2005 *Phys. Plasmas* **12**, 012505-1.

https://doi.org/10.1017/S0022377806006192 Published online by Cambridge University Press